

Computational Studies of the Aerophysical Characteristics on the Head Part of the Supersonic Body of Revolution During Flight Along Trajectories

Oleksandr M. Shyiko*, Olexii A. Obukhov and Igor V. Kopylyk

Sumy State University, Sumy, Ukraine

**E-mail:oleksandr.shyiko@yahoo.com*

ABSTRACT

The use of modern computer systems for calculating the aerophysical characteristics of supersonic bodies of revolution together with the calculation of the flight trajectory under conditions of continuously changing Mach and Reynolds numbers of the oncoming flow, the presence of transient regimes and non-isothermality in near-wall flows is often not possible due to the complexity of the organisation of the computational process. By using a number of integral methods for calculating inviscid flows and viscous compressible near-wall flows, taking into account the non isothermality and intermittency of the boundary layer, a method has been developed for calculating the friction and heating of supersonic bodies of revolution on the flight trajectory. On the basis of well-known flight experiments, the correlation dependences of the Reynolds numbers of the beginning of the transition on sharp cones were obtained and the method of corrections for spherical blunting of the head part was implemented. By calculating the intermittency function, the changeability of flow regimes in the boundary layer is established for a number of trajectories of the supersonic uncontrolled rocket projectile. Calculated dependences for aerodynamic friction, heat fluxes and projectile wall temperature on the flight time are obtained. The concept of combined calculation of aerophysical characteristics on the flight trajectory using numerical and integral methods is proposed.

Keywords: Rocket projectile; Flight trajectory; Laminar-turbulent transition; Intermittency function; Aerodynamic friction and heating; Integral methods and numerical simulation

1. INTRODUCTION

The currently existing software systems cannot provide the required accuracy of the aerophysical characteristics of high-Reynolds non-isothermal turbulent near-wall flows on the calculated flight path under conditions of continuously changing free stream parameters due to significant changes in flight altitude and speed, and aerodynamic heating of streamlined surfaces. The main difficulties are associated with modeling transient processes and non-isothermality in boundary layers. At the same time, the need to solve practical problems requires the calculation of aerophysical characteristics on the surfaces of various types of axisymmetric bodies of revolution in a wide range of sub-, trans-, and supersonic velocities. An important component in such calculations are friction and heating. To determine them, existing and newly developed software systems are used, which allow numerical simulation under conditions of a laminar-turbulent transition¹⁻⁴.

The most recognized and frequently used model of the laminar-turbulent transition is the γ - Re_{ot} SST⁵ model, which makes it possible to determine the position of the transition region in weakly compressible near-wall flows with a longitudinal pressure gradient. The use of this model for supersonic boundary layers is problematic because the model contains empirical correlations obtained at subsonic velocities. At the same time, the stabilising effect of compressibility

on the transition in supersonic boundary layers has been shown by the results of many theoretical and experimental studies⁶⁻¹⁰. The model also contradicts the well-known fact of the stabilizing effect of the unit Reynolds number on the transition^{6-7,10-11}, which is important for ballistic trajectories, where the unit Reynolds number of the oncoming flow can change significantly with height. A significant number of experimental and computational works demonstrate a significant effect of the spherical form of bluntness on the laminar-turbulent transition with the simultaneous stabilizing effect of the unit Reynolds number and flow compressibility^{12,17}.

The current state of practice in calculating the aerodynamic characteristics of supersonic axisymmetric bodies of revolution on a flight trajectory stimulated the authors to develop a technique and an efficient short algorithm that allow calculating friction and heating together with calculating the trajectory parameters under conditions of continuously changing Mach and Reynolds numbers of the oncoming flow. For this, the existing integral methods for calculating inviscid compressible flows and viscous compressible near-wall flows were used, taking into account non isothermality, longitudinal pressure gradient and intermittency of the boundary layer, data from field flight experiments.

The purpose of this work is to describe the developed technique and based on it a computational study of the flow regimes and associated aerophysical characteristics of near-wall boundary layers on the head of an axisymmetric body of

revolution with a spherical bluntness of the type of an unguided missile during flight along a trajectory. The study was carried out on the basis of existing flight data on the onset of a laminar-turbulent transition on sharp cones depending on the Mach number and unit Reynolds number at the outer boundary of the boundary layer and experimental data on the effect of spherical bluntness on the onset of a laminar-turbulent transition. The Reynolds numbers of the beginning of the transition are corrected for the spherical bluntness of the head part by the relative entropy increment on the shock wave. To calculate the aerodynamic friction and heat transfer of the boundary layer, integral methods verified by flight experiments¹⁸⁻¹⁹ were used. The turbulent viscosity was scaled by the intermittency function based on the empirical Chen-Tyson model modified during flight experiments¹⁹. The purpose of the study includes a comparative analysis of the obtained aerophysical characteristics and similar characteristics obtained using the CFD code for a viscous compressible fluid within the software package using the γ - Re_{θ} SST⁵ turbulence model.

2. METHODOLOGY

The values of the Reynolds numbers of the beginning of the laminar-turbulent transition necessary to establish the flow regime in the boundary layer were determined from the results of experiments on the flying sharp cones⁶⁻⁷, on the supersonic rocket aerophysical complex “Cloud” under the conditions of an operating solid propellant engine¹⁹ and from experiments in wind tunnels to determine the Reynolds numbers the beginning of the laminar-turbulent transition on cones with a spherical bluntness of the head part¹³. Flight data on the values of the Reynolds number of the beginning of the laminar-turbulent transition $Re_{e, tr}$ for the Mach number M_e at the outer boundary of the boundary layer within the limits $0.5 \leq M_e \leq 2.0$ at zero angle of attack were taken from report NASA⁶. In NASA’s flight experiment⁶ the 10° cone was installed in front of the nose of the F-15 aircraft. The reference²⁰ contains the photo of the experimental cone shown in Fig. 1(a). The values of the Reynolds number of the end of the laminar-turbulent transition $Re_{e, t}$ obtained during the flight experiment for the Mach number

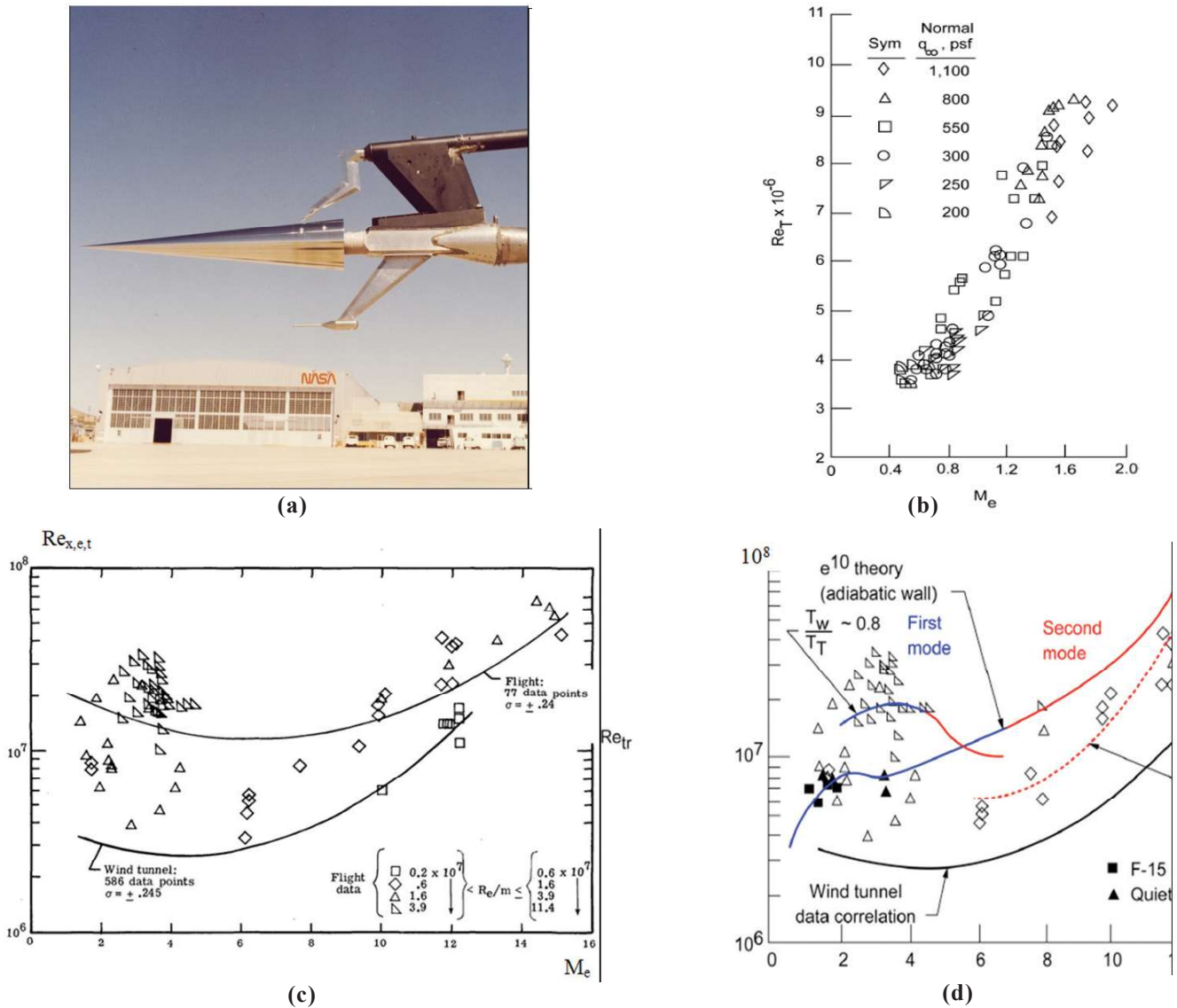


Figure 1. Flight data on laminar-turbulent transition on sharp cones: (a) experimental cone^{6,20}; (b) Reynolds numbers $Re_{e, T}$ of the end of the transition for $0.5 \leq M_e \leq 2.0$ ⁶; (c) Reynolds numbers $Re_{e, tr}$ of the beginning of the transition on sharp cones⁷; and (d) data on laminar boundary layer stability on sharp cones²⁰.

M_e at the outer boundary of the boundary layer at zero angle of attack⁶ are shown in Fig. 1(b). Using data⁶ about the average value of the ratio of the Reynolds number of the beginning of the transition $Re_{e,t}$ to the Reynolds number of the end of the transition $Re_{e,t}$ at a zero angle of attack as a function of the Mach number M_e at the outer boundary of the boundary layer, it was assumed that $Re_{e,t} = 0.85 \cdot Re_{e,T}$

Flight data on the values of the Reynolds number of the beginning of the laminar-turbulent transition at the outer boundary of the boundary layer $Re_{e,tr}$ within the Mach numbers $2.0 \leq M_e \leq 3.5$ were taken from study⁷ and are shown in Fig. 1(c).

The unified correlation of data on the change in the Reynolds number of the beginning of the laminar-turbulent transition on sharp cones at small angles of attack $Re_{e,tr}[R_{x,e,t}]$ in Fig. 1(c) depending on the Mach number M_e and the unit Reynolds number $Re_{e,1}[R_e/m]$ in Fig. 1(c) at the outer boundary of the boundary layer is compared with a similar correlation of data on the transition in wind tunnels. In the lower part of the figure, the boundary values of the ranges of variation of the unit Reynolds number R_e/m corresponding to individual correlations $R_{e,tr}$ are indicated. Shown in Fig. 1(b) and in Fig. 1(c) flight data has been included in a number of reviews of flight experiments on laminar-turbulent transition,

for example in²⁰⁻²¹. In Fig. 1(d) shows a fragment of a figure from a review²⁰, which shows generalised flight and calculated data on the stability of the laminar boundary layer on sharp cones. The figure simultaneously presents the results of flight experiments⁶⁻⁷, supplemented by the results of Malik's calculations on the stability of the laminar boundary layer²². In this case, the form of the calculated stability curve in the region of Mach numbers $0.5 \leq M_e \leq 3.5$ is important. The presented dependence shows a decrease in the stability of the boundary layer on the cone at Mach numbers on its outer boundary $M_e < 2.0$ and the presence of a local minimum at $M_e \approx 3.5$.

The results of flight experiments on the laminar-turbulent transition on the sharp cones were processed and approximated by a number of correlation dependences of the Reynolds number of the beginning of the laminar-turbulent transition $Re_{e,tr}$ on the Mach number M_e and the unit Reynolds number $Re_{e,1}$ at the outer boundary of the boundary layer. The resulting dependences $Re_{e,tr}(M_e)$ are shown in Fig. 2(a) and (b) as a series of correlation curves.

Correlation curves 1, 2, 3, 4 have their origin, respectively, at points b,c,d,e [Fig. 2(b)] and were set by the Table 1 as correlations of flight dependences $Re_{e,tr}$ on M_e for four ranges of values of the unit Reynolds number $Re_{e,1}$. Each correlation $Re_{e,tr}(M_e)$ in Fig. 2 corresponds to the average value of one

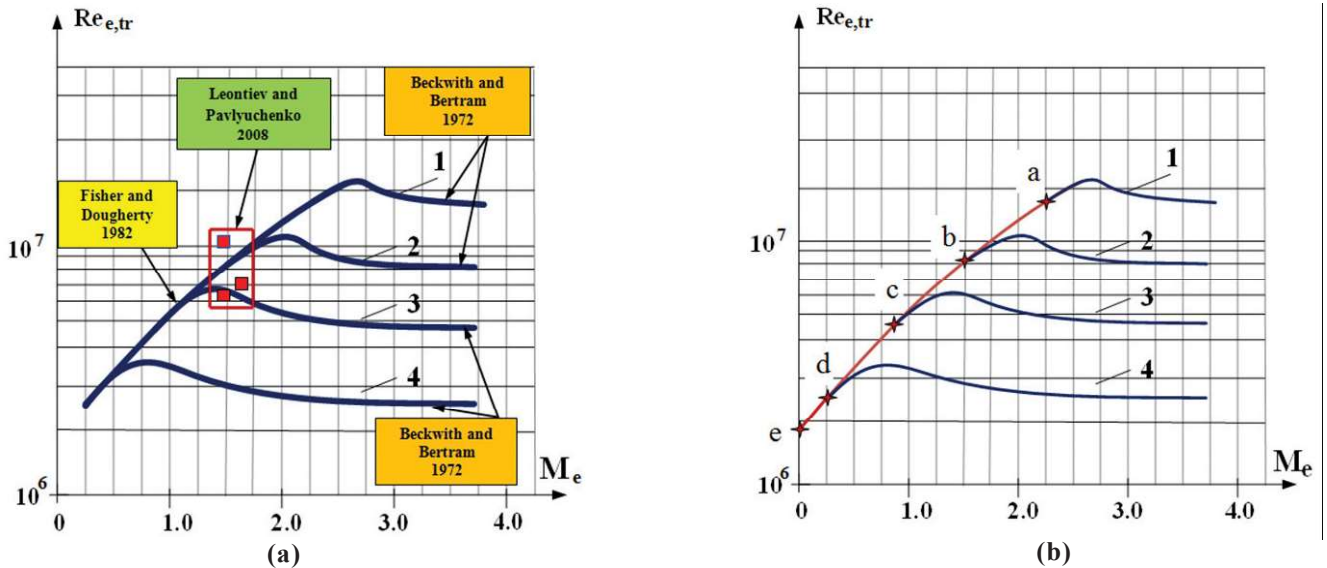


Figure 2. Correlations for the free-flight Reynolds number $Re_{e,tr}$ for sharp cones⁶⁻⁷.

Table 1. Numerical values of correlation dependences $Re_{e,tr}(M_e)$ on sharp cones⁶⁻⁷

Correlation number	M_e	1.5	1.625	1.75	1.875	2.0	2.25	2.5	2.625	2.75	3.0
	1	$Re_{e,tr} \cdot 10^{-6}$	8.5	9.25	10.3	12.5	14.0	17.0	20.0	22.0	21.0
2	M_e	0.875	1.0	1.25	1.5	1.75	2.0	2.25	2.5	2.75	3.0
	$Re_{e,tr} \cdot 10^{-6}$	4.5	5.2	6.5	8.25	9.5	10.2	9.75	8.5	8.25	8.0
3	M_e	0.25	0.5	0.875	1.0	1.25	1.375	1.5	1.75	2.0	2.25
	$Re_{e,tr} \cdot 10^{-6}$	2.5	3.25	4.5	5.0	6.0	6.2	6.0	5.5	5.2	5.0
4	M_e	0.0	0.25	0.50	0.75	1.0	1.25	1.5	1.75	2.0	2.25
	$Re_{e,tr} \cdot 10^{-6}$	1.8	2.5	3.0	3.3	3.25	3.0	2.8	2.7	2.6	2.5

of the ranges of values $Re_{e,1}$ in the study⁷. Correlation 1 matches meaning $Re_{e,1}=7.65 \cdot 10^7$, correlation 2– $Re_{e,1}=2.75 \cdot 10^7$, correlation 3– $Re_{e,1}=1.1 \cdot 10^7$, correlation 4– $Re_{e,1}=4.0 \cdot 10^6$. The location of the correlation curves in Fig. 2 corresponds to an increase in the Reynolds number $Re_{e,tr}$ of the beginning of the transition with growth $Re_{e,1}$. This trend is in line with research findings, for example¹³⁻¹⁵. In addition, each of the correlation curves 1-4 in Fig. 2 has a local minimum at $Me \approx 3.5$, which correlates with the results of the linear theory of boundary layer stability, for example²²⁻²³.

The use in this work of the results of flight experiments on sharp cones for calculating the characteristics of the boundary layer on a body of rotation with a small spherical bluntness is substantiated by the results of a number of theoretical and experimental studies. The results of some studies^{13,17} provide a basis for separately taking into account the influence of the unit Reynolds number and the bluntness radius when determining the beginning of the transition. The results of the experimental study¹³ at the Mach number of the oncoming flow $M_\infty=6.0$ in the range of the unit Reynolds number $Re_{\infty,1}=5.79 \cdot 10^6 \div 5.66 \cdot 10^7$ make it possible to determine the increase in the Reynolds number of the beginning of the laminar-turbulent transition $\Delta Re_{\infty,tr}$ at the radius of the spherical blunting of the model $R=0.5; 1.0 \div 8.0; 10.0; 12.0; 14.0$ mm compared to sharp cones, Fig. 3(a). The result of the approximation and further extrapolation of the study data¹³ on the cone with the spherical blunt radius of $R = 4.0$ millimeters $\Delta Re_{\infty,tr} = (\Delta Re_{\infty,tr})_{R=4}$ on the interval of unit Reynolds numbers $Re_{\infty,1}$ in the study⁷ is shown in Fig. 3(b).

In order to take into account the effect of the bluntness radius at the Mach numbers of the oncoming supersonic flow other than $M_\infty = 6.0$, the value of the relative entropy increment at the shock wave was used in the form $K_s = \Delta S / \Delta S_6$, where ΔS is the entropy increment on the shock wave at the current Mach numbers M_∞ of the in-stream flow, ΔS_6 is the increment of entropy at the shock wave at the Mach number $M_\infty = 6.0$. The corresponding increments of entropy²⁴ $\Delta S = -R \cdot \ln(v_0)$ and $\Delta S_6 = -R \cdot \ln(v_0)_6$ can be calculated at the dependences containing

the values of the recovery coefficient of the total pressure on the shock wave $v_0 = p'_0/p_0$ at the current Mach numbers M_∞ and $(v_0)_6 = (p'_0/p_0)_6$ at $M_\infty = 6.0$, where p'_0 – the total pressure behind the disconnected shock wave in front of the blunt body, p_0 – the total pressure in the freestream²⁴. The real process of increasing entropy ($\Delta S > 0$) corresponds to a supersonic flow ($M_\infty \geq 1.0$). In this case, at $M_\infty \geq 1.0$ $K_s = \Delta S / \Delta S_6 = \ln(v_0) / \ln(v_0)_6$. The value of the relative increment of entropy at the shock wave takes on a value $K_s = 1$ at $M_\infty = 6.0$ and $K_s = 0$ at $M_\infty = 1.0$. The total pressure p'_0 can be found as the pressure at the point of complete stagnation (at the critical point) of a blunt surface located behind the direct shock wave. In this case, the expression for the recovery factor of the total pressure on the shock has the form²⁴ ($M_\infty = M_1 \geq 1.0$, M_1 – Mach number of the supersonic flow ahead of the shock wave)

$$v_0 = p'_0/p_0 = \left\{ \left[\frac{(k+1)M_\infty^2}{2 + (k-1)M_\infty^2} \right] \right\}^{k/(k-1)} \cdot \left\{ \frac{[k+1]}{[2kM_\infty^2 - (k-1)]} \right\}^{1/(k-1)} \quad (1)$$

Natural logarithms of the recovery factor of the total pressure at the direct shock wave at $k = 1.4$ and $M_\infty \geq 1.0$ will be equal to:

$$\ln(v_0) = 3.5 \ln\left(\frac{6M_\infty^2}{5 + M_\infty^2}\right) + 2.5 \ln\left(\frac{6}{7M_\infty^2 - 1}\right); \quad (2)$$

$$\ln(v_0)_6 = -3.518$$

The Reynolds number of the beginning of the transition, calculated from the parameters at the outer boundary of the boundary layer, taking into account corrections for the spherical bluntness of the head part, was determined as follows:

$$Re_{e,tr} = (Re_{e,tr})_{sh.} + \Delta(Re_{e,tr})_{R=4mm} \cdot K_s \quad (3)$$

To calculate the local coefficients of friction and heat transfer of the boundary layers on the calculated flight trajectory, the dependences verified during the flight experiment were used. In particular, to obtain the calculated values of the local coefficients of friction C_{fl} and heat transfer α_L on the surface of the rocket complex¹⁹, taking into account non isothermality and compressibility in the case of a laminar boundary layer,

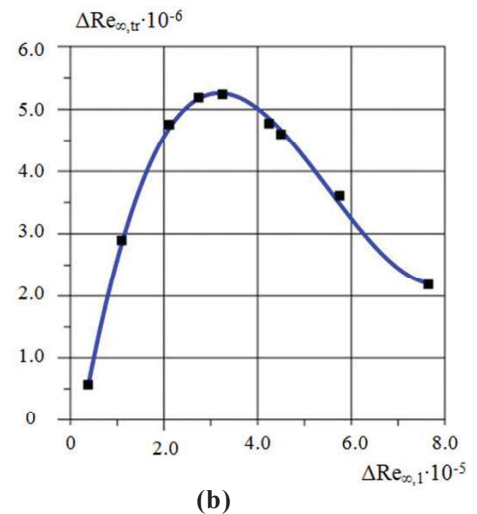
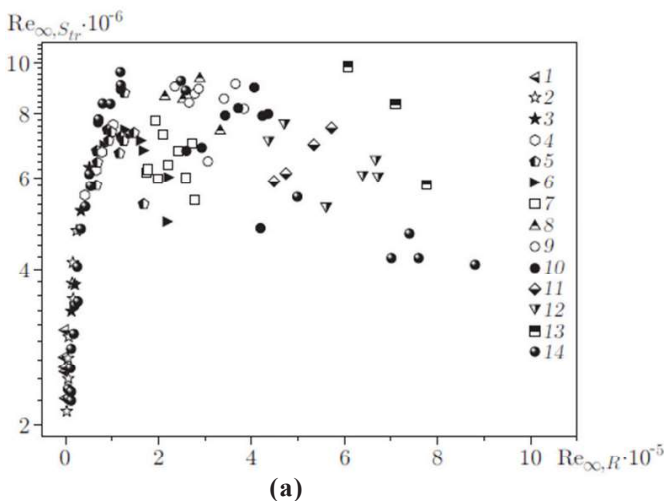


Figure 3. The effect of spherical bluntness on the Reynolds number $Re_{e,tr}$ of the beginning of the laminar-turbulent transition for a cone with at the Mach number $M_\infty=6.0$ according to the study¹³: (a) Experimental transition Reynolds numbers for cone with bluntness R ($6-R=4$ mm; $1-R=0$)¹³; and (b) Approximation of the data¹³ on the increase in the Reynolds numbers of transition for cone with $R=4$ mm.

the known dependences²⁵ for the longitudinal flow around a flat plate were used:

$$\begin{aligned} C_{fL}/2 &= C_{fL0}/2 \cdot \psi^{-0.11} \cdot \psi^*^{-0.04}; \\ C_{fL0}/2 &= 0.332/\sqrt{\text{Re}_{e,x}}; \alpha_L = \text{St}_L \cdot \rho_e \cdot u_e \cdot c_{p,e}; \\ \text{St}_L &= 0.332/\sqrt{\text{Re}_{x,e}} \cdot \sqrt{\psi_L}/\text{Pr}^{2/3}; \psi_L = \psi^{-0.22} \cdot \psi^*^{-0.08} \end{aligned} \quad (4)$$

where, $C_{fL0}/2$ – local coefficient of friction for the laminar boundary layer of incompressible fluid on the flat heat-insulated plate; $\text{Re}_{e,x} = (\rho_e \cdot u_e \cdot X)/\mu_e$ – Reynolds number at the outer boundary of the boundary layer, determined taking into account the existing pressure gradient; St_L – Stanton number for laminar boundary layer; ρ_e, u_e, μ_e – density, velocity and coefficient of dynamic viscosity at the outer boundary of the boundary layer; X – longitudinal coordinate of the surface point; $c_{p,e}$ – heat capacity of air at constant pressure at the outer boundary of the boundary layer; ψ, ψ^* – parameters that take into account the non-isothermal nature of the flow around a flat plate by a laminar boundary layer; $\psi = T_w/T_{r,e,L}$ – temperature factor, $\psi^* = T_{r,e,L}/T_e$ – kinetic temperature factor; T_e – temperature at the outer boundary of the boundary layer; $T_{r,e,L} = T_e \cdot [1 + r_L \cdot (k-1)/2 \cdot M_e^2]$ – equilibrium wall temperature in the case of a laminar boundary layer, determined from the parameters T_e and M_e at the outer boundary of the boundary layer; $r_L = \sqrt{\text{Pr}}$; Pr – Prandtl number; $k = 1.4$ – adiabatic index; M_e – Mach number at the outer boundary of the boundary layer.

To calculate the local coefficients of friction C_{fT} and heat transfer α_T in the boundary layer on the surface of the rocket complex¹⁹ in case of the turbulent boundary layer, the integral method was used based on the results of the asymptotic theory of a turbulent boundary layer¹⁸:

$$\begin{aligned} C_{fT}/2 &= C_{fT0}/2 \cdot (\Psi_M \cdot \Psi_t)^{0.8} \cdot (\mu_w/\mu_e)^{0.2}; \\ C_{fT0}/2 &= 0.0288 \cdot \text{Re}_{e,x}^{-0.2}; \alpha_T = \text{St}_T \cdot \rho_e \cdot u_e \cdot c_{p,e}; \\ \text{St}_T &= C_{fT}/2 \cdot \text{Pr}^{-2/3} \end{aligned} \quad (5)$$

C_{fT0} – local coefficient of friction for a turbulent boundary layer of incompressible fluid on the flat heat-insulated plate; St_T – Stanton number for a turbulent boundary layer taking into account the existing pressure gradient; μ_w – the value of the coefficient of dynamic viscosity of air at wall temperature T_w ; Ψ_M and Ψ_t – relative laws of frictional resistance, taking into account, respectively, compressibility and non-isothermality in the boundary layer.

$$\begin{aligned} \Psi_M &= \left[\arctg \left(M_e \sqrt{r_T (k-1)/2} \right) \right] / \left[M_e \sqrt{r_T (k-1)/2} \right]^2; \\ \Psi_t &= \left[2.0 / \left(\sqrt{T_w/T_{r,e,T}} + 1 \right) \right]^2 \end{aligned} \quad (6)$$

where $T_{r,e,T} = T_e \cdot [1 + r_T \cdot (k-1)/2 \cdot M_e^2]$ – equilibrium wall temperature in the case of a turbulent boundary layer; $r_T = \sqrt[3]{\text{Pr}}$ – coefficient of recovery for a turbulent boundary layer.

The calculation of local values of the heat transfer coefficient α under conditions of a laminar-turbulent transition was carried out using the theory of turbulent spots²⁶. In work²⁷ based on a generalization of the results of experimental studies of the laminar-turbulent transition in supersonic wind tunnels, the dependence of the rate of formation of turbulent spots on the Reynolds number of the transition and on the Mach number was found. The expression is obtained for the intermittency function of the laminar-turbulent low-gradient boundary layer on a thermally insulated surface of axisymmetric bodies of rotation. In the work¹⁹, a modified formula for the intermittency function γ is given in the form:

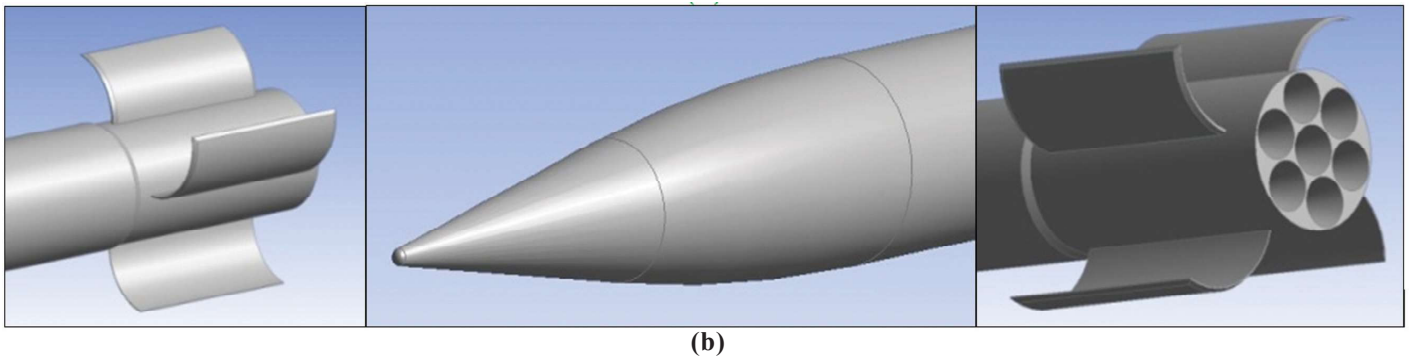
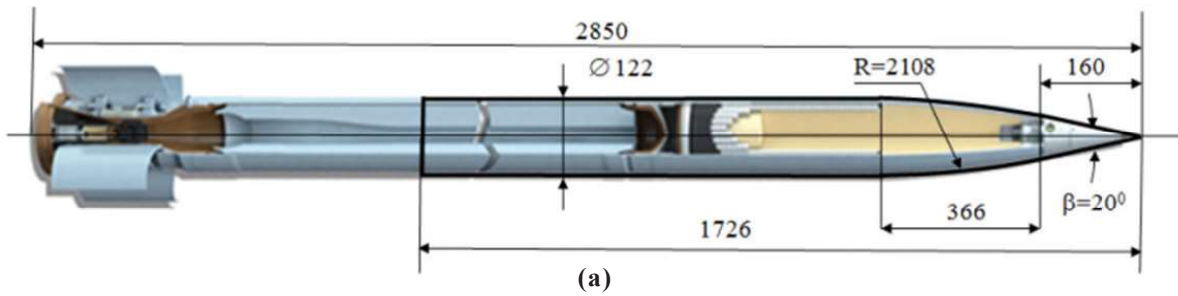


Figure 4. Main dimensions (a) and computer visualisation (b) of the external contours of the uncontrolled rocket projectile of the M21-OF type⁴.

$$\gamma = 1.0 - \exp\left\{-\left(3.507/A^2\right) \operatorname{Re}_{e, \text{tr}}^{-1.34} \left(u_e \rho_e / \mu_e\right)^2 \cdot \left(\mu_{e, \text{tr}} / u_{e, \text{tr}} / \rho_{e, \text{tr}}\right)^2 \cdot \left(\operatorname{Re}_{e, x} - \operatorname{Re}_{e, \text{tr}}\right)^2\right\} \quad (7)$$

tr – index referring to the parameters at the beginning of the transition.

In the laminar-turbulent transition zone, the calculation of the local friction coefficient C_f the Stanton number St and the heat transfer coefficient α was carried out using a linear-combination model of Narasimha²⁸ tested in a flight experiment¹⁹ for the case of a weakly gradient flow:

$$C_f = C_{fL}(1-\gamma) + C_{fT} \cdot \gamma, \quad St = St_L(1-\gamma) + St_T \cdot \gamma, \quad \alpha = \alpha_L(1-\gamma) + \alpha_T \cdot \gamma \quad (8)$$

where, C_{fL} , St_L , α_L and C_{fT} , St_T , α_T are the local coefficients of friction, Stanton numbers and heat transfer coefficients, respectively, for laminar and turbulent flow in the boundary layer; γ – function of intermittency according to dependence (7).

Aerodynamic heating of the surface of the projectile on the calculated flight trajectory was carried out using the dependencies verified by the flight experiment. In the study¹⁹ the calculations of the wall temperature of aero physical missile complex “Cloud” were carried out on the basis of a physical model of the «thin wall» and the corresponding differential heat balance eqn: $\rho_w c_w \delta_w \cdot dT_w / d\tau = \alpha \cdot (T_{r,e} - T_w) - \epsilon_w \cdot \sigma_0 \cdot T_w^4$ where, $\rho_w, c_w, \delta_w, T_w$ – respectively, density, heat capacity, wall thickness, wall temperature, ϵ_w – degree of emissivity of the surface of the head part; σ_0 – Stefan-Boltzmann constant; $T_{r,e}$ – equilibrium wall temperature, determined from the parameters at the outer boundary of the boundary layer; α – coefficient of heat transfer by convection to the streamlined surface. According to the “thin wall” model, the wall material is heated evenly over the entire thickness. In the case of a continuous filling of the space inside the body of a flight object with a dense substance and a short-term process of aerodynamic heating, the filling substance can be considered as a heat insulator for a thin wall of the object’s body, and the

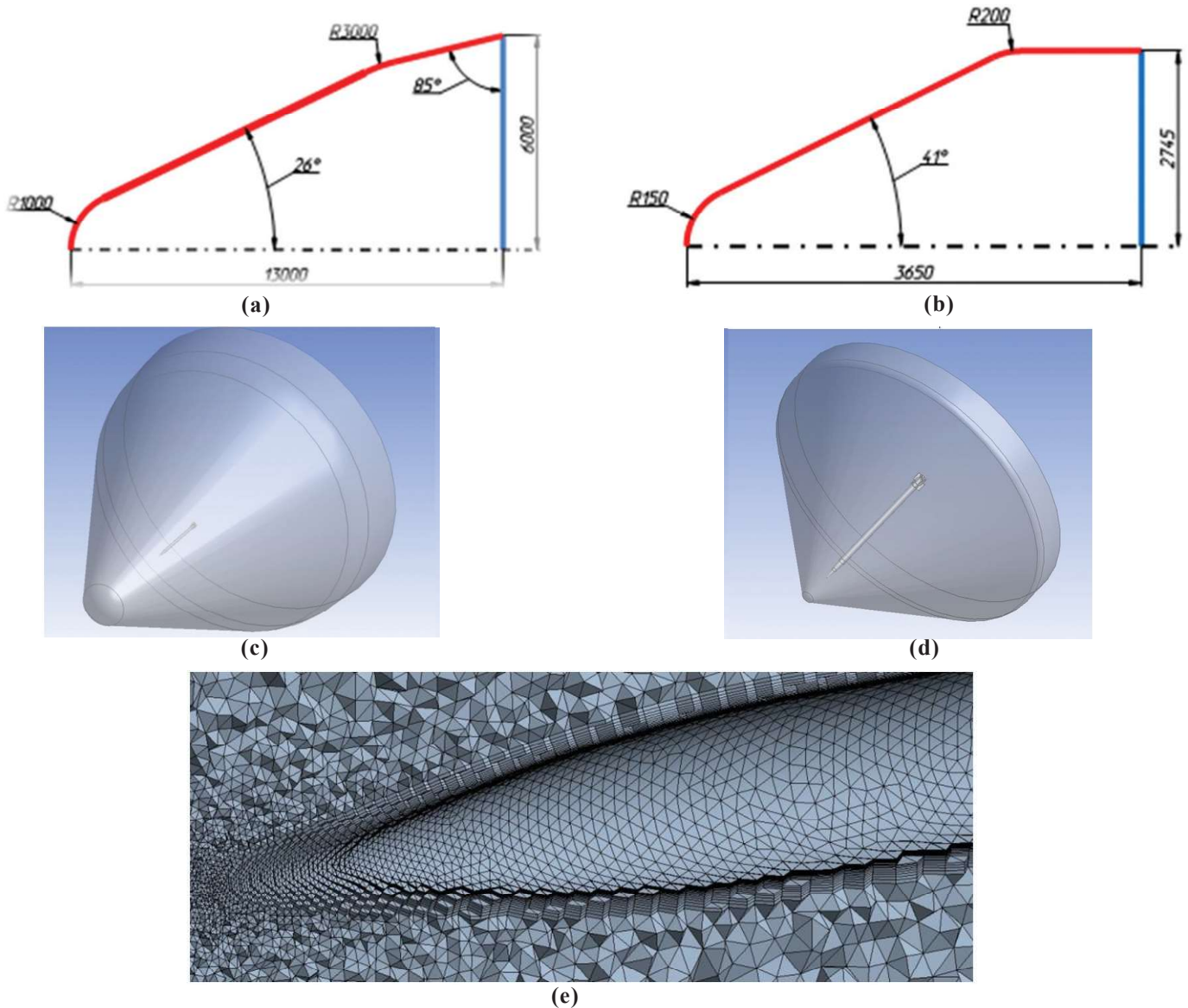


Figure 5. Geometric parameters and type of computational domain: at subsonic and transonic velocities (a, c); at supersonic velocities (b,d); fragment of the computational grid (e).

heat balance equation can be used in the same form. According to the algorithm used, the calculated projectile surface was divided along the length into sections 0.01 mtr wide. Within each section, the flow parameters at the outer boundary of the boundary layer and the wall temperature were considered constant and were calculated at each numerical integration time step together with the flight trajectory parameters. The “thin wall” model was used in the absence of heat exchange between adjacent sections of the surface of the projectile. The wall thickness was 2.0 mm. The wall material is steel.

The calculated trajectory of the projectile was determined by numerical integration over time of the system of equations of motion in the active and passive flight segments. For the calculation, the consumption and thrust characteristics of the engine of the M21-OF projectile of the BM-21 «Grad» rocket system were taken²⁹.

The coefficients of the acting aerodynamic forces of frictional drag, pressure drag, bottom drag, necessary for calculating the trajectory of flight, were preliminarily determined from the outer contours of the projectile (Fig. 4) depending on the Mach number of the oncoming flow M_∞ by numerical integration of the Navier-Stokes equations in the range sub-, trans- and supersonic velocities⁴. The system of ordinary nonlinear differential equations used, which includes the motion equations of the body of rotation along a trajectory and the eqn. of heating a “thin wall” of its surface, was solved numerically by the Runge-Kutta method ($h=0.05$ of sec.).

The calculation of the parameters on the outer boundary of the boundary layer at each calculated point of the trajectory within each section of the projectile surface was carried out in the following sequence. First, by numerical integration of the system of differential equations of the projectile motion, the height and velocity of its flight were determined. The Mach number of the oncoming flow was determined from the known flight velocity and the parameters of the standard atmosphere at the known flight altitude. Next, the distribution of the pressure coefficient $\bar{p} = (p_e - p_\infty)/q_\infty$ along the surface of the projectile was calculated (p_e is the pressure at the outer boundary of the boundary layer, q_∞ is the velocity head of the counter flow). The calculation \bar{p} was carried out at supersonic and subsonic flight velocity by solving the equation for the velocity perturbation potential ϕ' when a compressible fluid flows around a thin body in a linear approximation using the sources method. For known values of M_∞ , p_∞ and \bar{p} , the values of pressure p_e and Mach number M_e at the outer boundary of the boundary layer were calculated taking into account the losses at the shock wave. Then, using the known isentropic relations^{24,25}, the density ρ_e and the temperature T_e at the outer boundary of the boundary layer were calculated. For known values of p_e , ρ_e and T_e , the velocity of sound a_e and viscosity μ_e , and then the velocity u_e and the Reynolds number $Re_{x,e}$ at the outer boundary of the boundary layer were determined.

Subsonic and supersonic flow around a projectile was simulated by the ANSYS CFX software package using the γ - Re_{θ} SST^{5,30} turbulence model. The geometry of the research object was created in the Ansys Design Modeler module. In Fig. 4(b) shows fragments of computer visualization of the research object. Two geometries of the computational domain

were created. The first geometry is for studying subsonic and transonic flow [Fig. 5(a,c)], the second is for studying supersonic flow [Fig. 5(b,d)]. The “Enter” conditions were set at the boundaries marked in red, the “Exit” conditions – at the boundaries marked in blue. The fundamental difference between the created geometries of the computational domains is that for subsonic and transonic flow it is necessary to ensure attenuation of acoustic waves before the “Enter” boundary conditions. When constructing the computational domain for supersonic flow, the requirement that a shock wave should not be superimposed on the “Enter” boundary conditions was taken into account. The computational grids were created in the Ansys Meshing module and consisted of tetrahedra for the main flow and prisms for the boundary layer.

When constructing computational grids, the following quality criteria were ensured. The minimum cell node angle (Orthogonal Angle) – $>20^\circ$. The extent of the cell (the ratio of the length of the maximum edge to the length of the smallest edge of the cell) in percentage (Aspect Ratio) – <1000 . The maximum relative increase in a cell in a nearby layer, reflected in percentage (Expansion Factor) – <100 . Setting up the computational grid in the boundary layer. First Layer Height – $1.2e-3$ mm. Number of layers – 50. Growth Rate – 1.17. General parameters of the computational grid for subsonic and transonic flow: Total Number of Nodes – 6598158; Total Number of Elements – 16468498. General parameters of the computational grid for supersonic flow: Total Number of Nodes – 10173776; Total Number of Elements – 25733671. Setting the boundary conditions “Wall”: Smooth wall, Adiabatic. The fragment of the computational grid in the area of the head part of the object is shown in Fig. 5(e). The value of the time integration step in the studied range of Mach numbers varied for each Mach number from 0.0075 s at $M_\infty=0.1$ to $7.5e-6$ s at $M_\infty=2.8$. The values of the y^+ parameter were controlled in the Results module and on most of the projectile surface did not exceed the value 2.0 recommended for the SST turbulence model⁵.

3. RESULT

Figure 6(a) shows the calculated dependences of the Mach number M_∞ of the oncoming flow on the flight time T for various values of the angle of inclination of the launch guides $\theta_0 = 15^\circ; 30^\circ; 45^\circ$. In Fig. 6(b) shows the calculated dependences of the distribution of the pressure coefficient \bar{p} along the length of the projectile. In Fig. 6(c) shows the calculated dependences of the static pressure P_e on the flight time T along the trajectory for three points on the surface of the projectile, indicating the existence of a negative pressure gradient on the surface of the projectile. Similar calculated dependences for temperature T_e and velocity u_e at the outer boundary of the boundary layer are shown in Fig. 6(d) and Fig. 6(e). The calculated dependences of $Re_{x,e}$ on time T at three points along the length of the projectile are shown in Fig. 6(f). With known flow parameters at the outer boundary of the boundary layer, the calculation of the Mach number M_e and unit Reynolds number $Re_{e,1}$ at its outer boundary was performed. Figure 7 shows the dependencies illustrating the results of calculations to determine the flow regimes in the boundary layer. Figure 7(a) and Fig. 7(b) shows

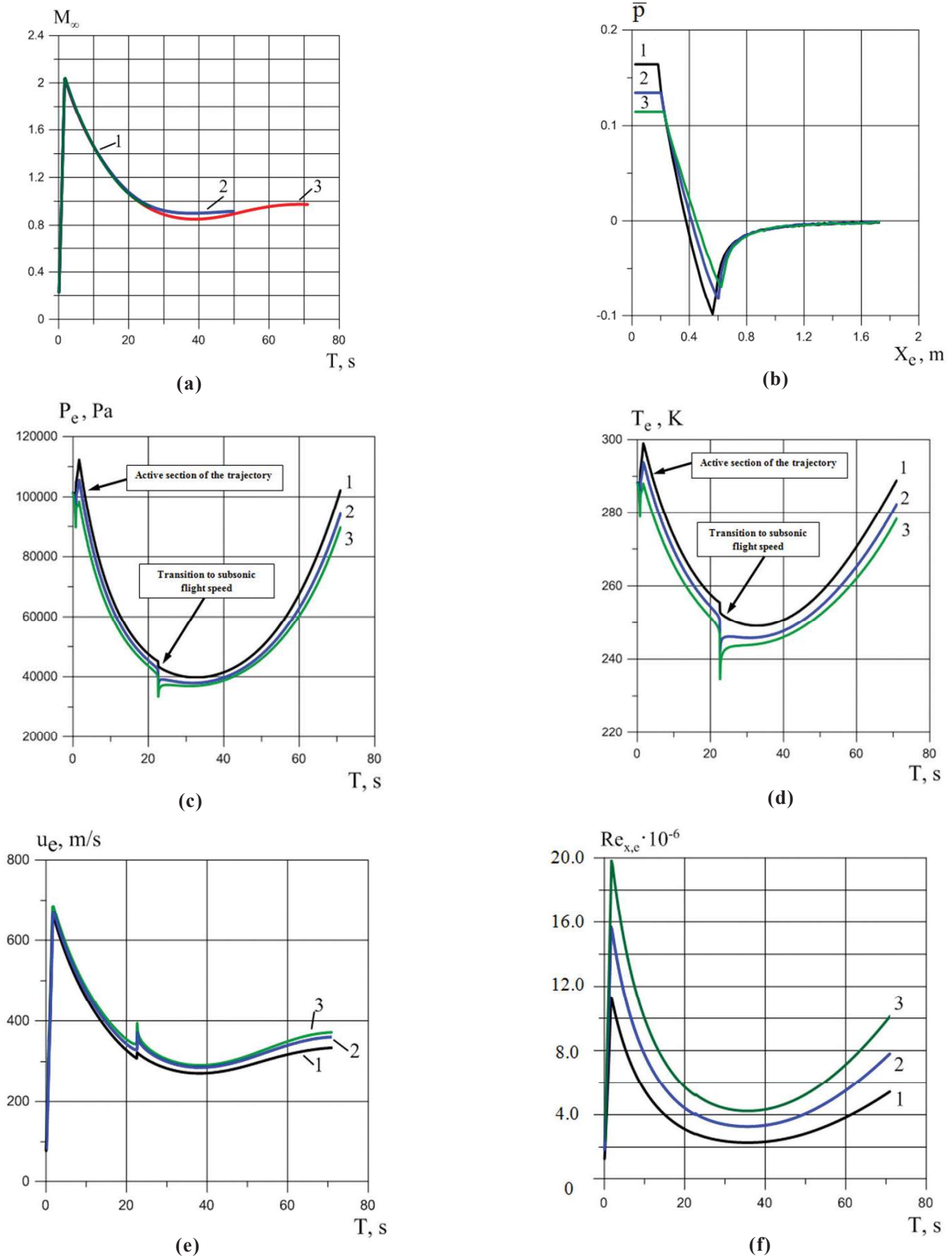


Figure 6. Flow parameters at the outer boundary of the boundary layer, (a) Mach number M_∞ from the flight time T at the angles of inclination of the starting guides $\theta_0 = 15^\circ$ (1), $\theta_0 = 30^\circ$ (2), $\theta_0 = 45^\circ$ (3), (b) Pressure coefficient \bar{p} along the length of the projectile at different Mach numbers (1- $M_\infty = 1.2$; 2- $M_\infty = 1.6$; 3- $M_\infty = 2.0$); (c) static pressure P_e from the flight time T (1- $X = 0.24$ m; 2- $X = 0.34$ m; 3- $X = 0.44$ m); (d) temperature T_e from the flight time T (1- $X = 0.24$ m; 2- $X = 0.34$ m; 3- $X = 0.44$ m); (e) velocity u_e from the flight time T (1- $X = 0.24$ m; 2- $X = 0.34$ m; 3- $X = 0.44$ m); and (f) Reynolds number $Re_{x,e}$ from the time T (1- $X = 0.24$ m; 2- $X = 0.34$ m; 3- $X = 0.44$ m).

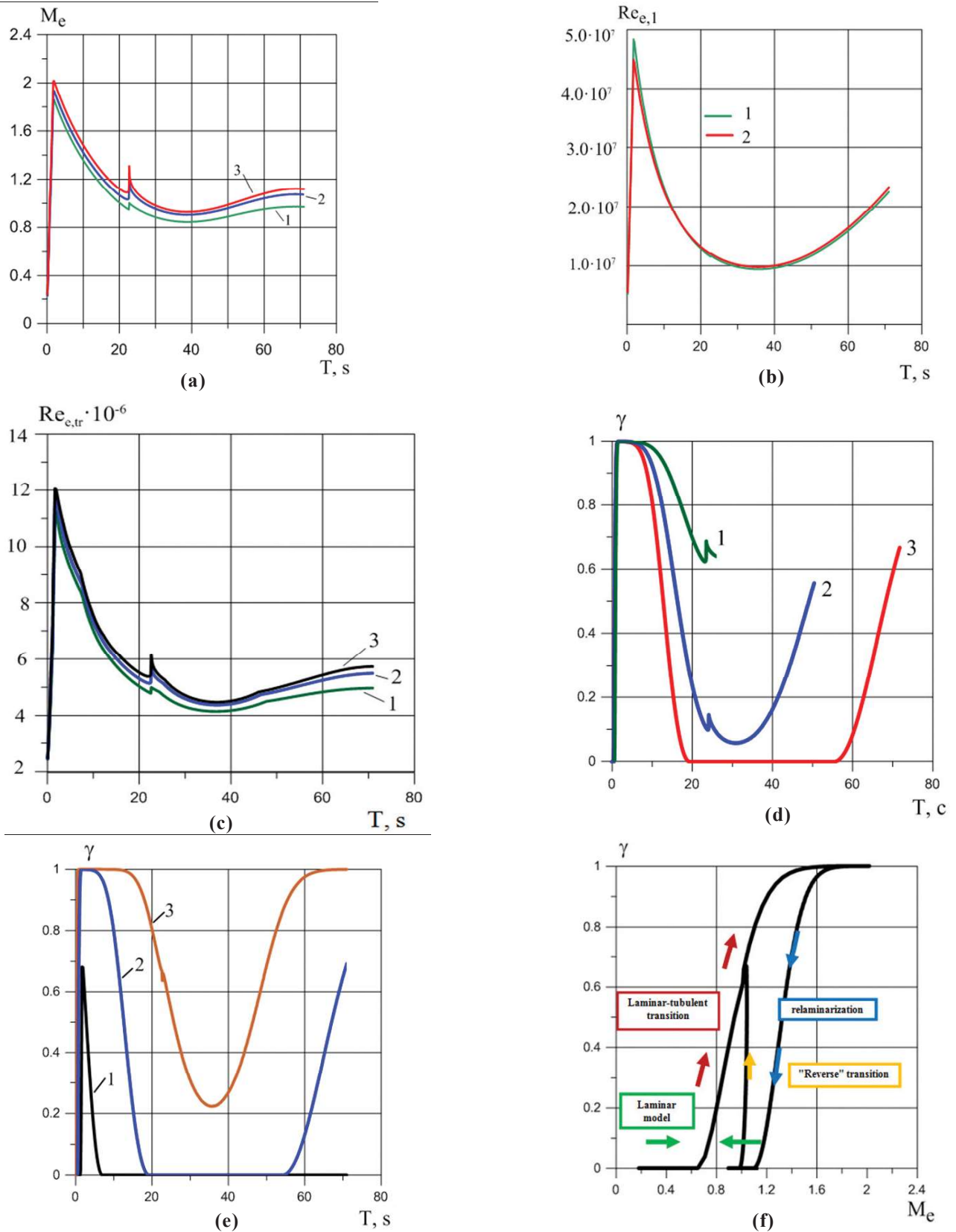


Figure 7. Dependencies illustrating the results of calculations related to the determination of flow regimes in the boundary layer, a) Mach number M_e from the time T (1- $X=0.24$ m; 2- $X=0.34$ m; 3- $X=0.44$ m); (b) Unit Reynolds number $Re_{e,1}$ from the time T (1- $X=0.24$ m; 2- $X=0.44$ m); (c) Reynolds number of the beginning of the transition $Re_{e,tr}$ from the time T (1- $X=0.24$ m; 2- $X=0.34$ m; 3- $X=0.44$ m); (d) intermittency function γ from the time T for $X = 0.340$ m (1- $\theta_0=15^\circ$; 2- $\theta_0=30^\circ$; 3- $\theta_0=45^\circ$); (e) Intermittency function γ from the time of flight T (1- $X = 0.24$ m; 2- $X = 0.34$ m; 3- $X = 0.44$ m); and (f) intermittency function γ from the Mach number M_e at the outer boundary of the boundary layer ($X = 0.34$ m).

the corresponding calculated dependences of the Mach number M_e and the unit Reynolds number $Re_{e,1}$ at three points along the length of the projectile on the time T of its flight along the trajectory. With known values of the numbers M_e and $Re_{e,1}$, according to the correlation dependences of Table 1, the value of the Reynolds number $(Re_{e,tr})_{sh}$ of the beginning of the laminar-turbulent transition at a point on the surface of the head part in the form of a pointed cone was determined.

Reynolds number of the transition, taking into account corrections for the spherical bluntness of the head part $Re_{e,tr}$ was calculated from dependence (3). In Fig. 7(c) shows the calculated dependences of the transition Reynolds number $Re_{e,tr}$ at the same three points along the length of the projectile on the flight time T . The obtained values of $Re_{e,tr}$ were used to determine the beginning of the laminar-turbulent transition zone and calculate the intermittency coefficient γ in this zone using formula (7). The calculated data on the change in the intermittency function γ when the projectile moves along the trajectory in the presence of aerodynamic heating is advisable to use to establish aerophysical effects for this object on the streamlined surface. In particular, in Fig. 7(d) shows the calculated dependences of the intermittency function γ at a projectile surface point with a longitudinal coordinate $X = 340$ mm on time T during flight along three calculated trajectories with initial angles of inclination of the launch guides $\theta_0 = 15^\circ, 30^\circ, 45^\circ$.

Curves 1 and 2, corresponding to $\theta_0 = 15^\circ$ and $\theta_0 = 30^\circ$, show the moments of transition to subsonic flight velocity. The values of the intermittency coefficient $0 < \gamma < 1.0$ correspond to the transitional flow regime in the boundary layer. In Fig. 7(e) shows the calculated dependences of the intermittency coefficient γ of the near-wall boundary layer on the flight time T along the trajectory for three points on the surface of the projectile head part at the angle of inclination of the launch guides $\theta_0 = 45^\circ$. In Fig. 7(f) shows the calculated dependence of the intermittency function γ on the Mach number M_e at the outer boundary of the boundary layer at the point of the projectile surface with the coordinate $X = 0.340$ m when the projectile is flying along the trajectory with the angle

of inclination of the launch guides $\theta_0 = 45^\circ$. It can be seen that at the point with the coordinate $X = 0.340$ m during a significant part of the flight time, the processes of laminar-turbulent transition and relaminarisation in the boundary layer occur. The reason for the relaminarisation and the subsequent “reverse” of the laminar-turbulent transition is a decrease in the Reynolds number at the outer boundary of the boundary layer below the critical one and its subsequent growth under the conditions of a “natural” transition. This is due to the ascent to an altitude with a simultaneous decrease in flight velocity and further return to denser layers of the atmosphere with a simultaneous increase in flight velocity. The use of formula (7) for the intermittency function γ of the near-wall boundary layer both in the zone of the laminar-turbulent transition and relaminarisation, firstly, can be justified by the existence of the moderate negative pressure gradient on the surface of the head part of the projectile. Second, by a continuous monotonic change in the parameters of the freestream over relatively long periods of flight time along the trajectory.

Figure 8 illustrates the effect of spherical bluntness on the Reynolds number $Re_{e,tr}$ of the beginning of a laminar-turbulent transition. In Fig. 8(a) shows the dependence of the relative increment of entropy $K_s = \Delta S / \Delta S_0$ at the head shock wave during flight along the trajectory on the Mach number M_∞ . In Fig. 8(b) shows the dependence of the increment of the Reynolds number $\Delta Re_{e,tr}$ of the beginning of the laminar-turbulent transition from the flight time T (point $X = 340$ mm).

Due to the intermittency of the flow in the boundary layer, the calculation of the local values of the friction and heat transfer in the transition zone was carried out according to dependencies (8). The change in the Stanton number St during the flight time T at three calculated points of the projectile surface at $\theta_0 = 45^\circ$ is shown in Fig. 9(a). In Fig. 9(b) shows the calculated dependences of the heat transfer coefficient α on the flight time T on the projectile surface. As can be seen, the highest values of the heat transfer coefficient α reaches at the end of the active section of the trajectory at the point with the coordinate $X = 340$ mm. In Fig. 9(c) shows the dependences of the projectile wall temperature T_w from the flight time, obtained

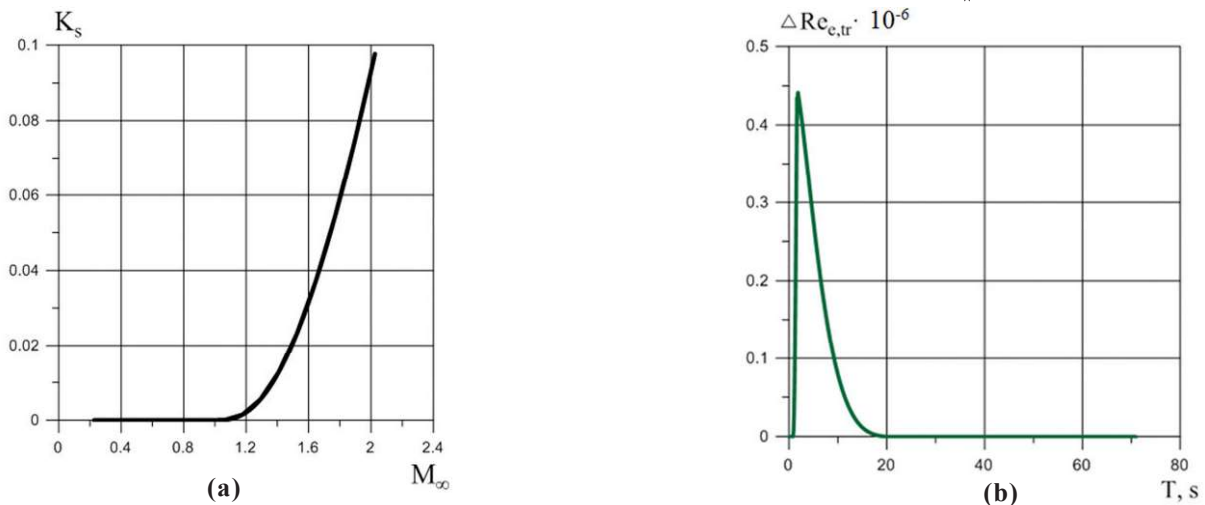


Figure 8. Influence of spherical bluntness on the Reynolds number $Re_{e,tr}$ on the calculated flight trajectory for bluntness radius $R=4$ mm, a) relative increment of the entropy K_s ; and b) Increment $\Delta Re_{e,tr}$ Reynolds number from the Mach number M_∞ $Re_{e,tr}$ from time T ($X = 0.34$ m).

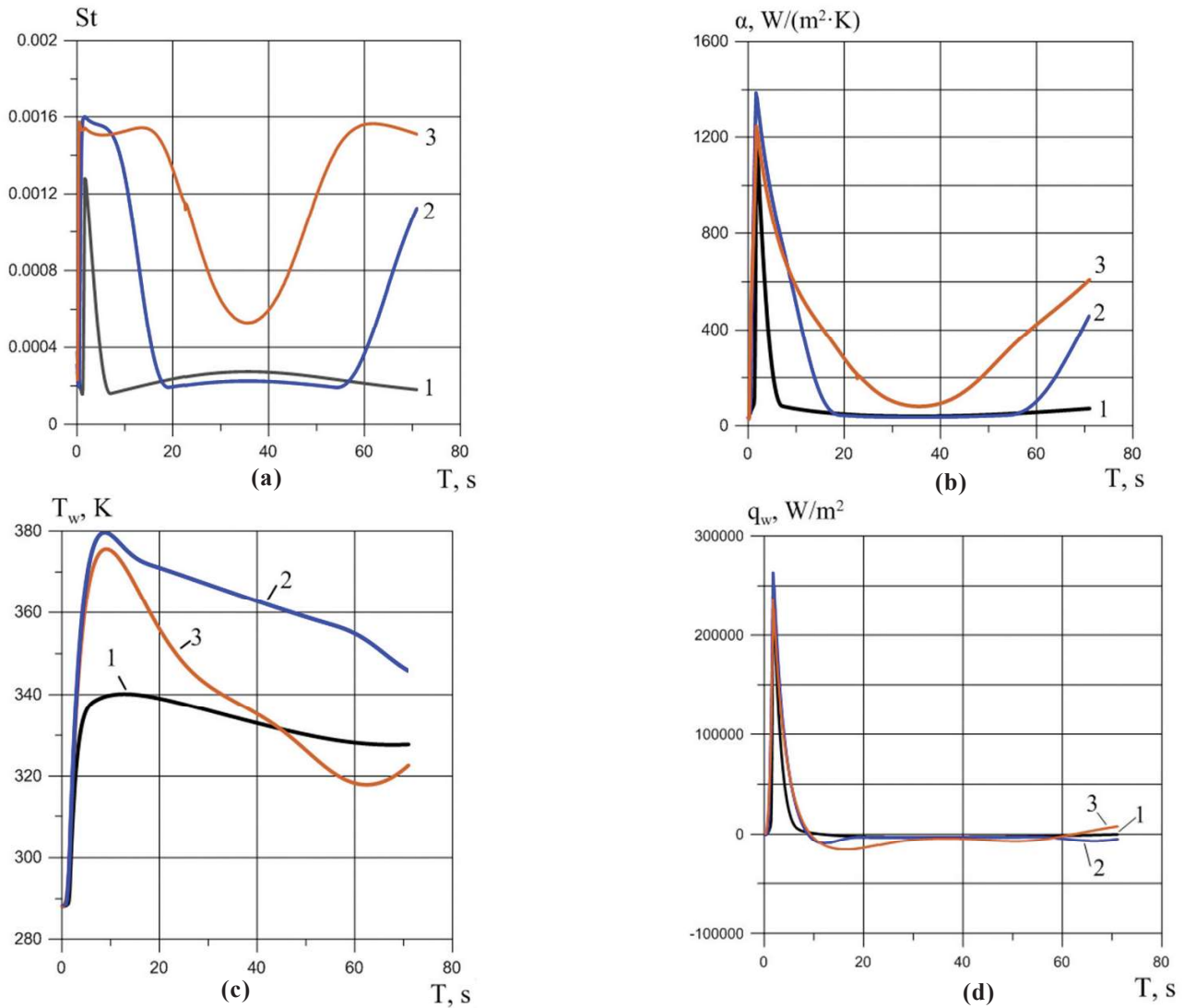


Figure 9. Results of calculating the heat transfer of the boundary layer from the time T , (a) change in the Stanton number St (1- $X=0.24$ m; 2- $X=0.34$ m;3- $X=0.44$ m); (b) Change in the heat transfer coefficient α (1- $X=0.24$ m; 2- $X=0.34$ m;3- $X=0.44$ m); c) change in the wall temperature T_w (1- $X=0.24$ m; 2- $X=0.34$ m;3- $X=0.44$ m); and (d) heat flux to the streamlined surface q_w (1- $X=0.24$ m; 2- $X=0.34$ m;3- $X=0.44$ m).

by integrating of the differential equation of the “thin wall”. The calculation results show that up to approximately the 10-th second of the flight, the surface of the projectile heats up at all control points. When higher and colder layers of the atmosphere are reached with a simultaneous decrease in flight velocity, the surface of the projectile cools, Fig. 9(c). In Fig. (d) shows the calculated dependences of the heat flux q_w to the streamlined surface at three of its points on the time T of the projectile’s flight along the trajectory at $\theta_0=45^\circ$. It can be seen that after approximately the 7th second of flight, the heat flux q_w to the streamlined surface becomes negative.

The calculation of the aerodynamic friction resistance, in contrast to the calculation of the aerodynamic heating of the surface of the projectile, was carried out along the entire length of its head part for a number of fixed values of the Mach numbers M_∞ of the oncoming flow. The calculation was performed on the active part of the flight trajectory with an increase in the Mach number M_∞ . In Fig. 10(a) shows the distribution of the local coefficient of friction C_f along the length of the projectile head part at various Mach numbers M_∞ of the counter subsonic

and supersonic flow on the calculated flight trajectory with the initial angle of inclination of the launch guides $\theta_0=45^\circ$. Fig. 10(a) shows the stabilizing effect of the unit Reynolds number of the oncoming flow. With an increase in the Mach number M_∞ , the beginning of the transition practically does not shift towards the nose of the head part but is localised in a rather narrow region of its surface. This is explained by the fact that the values of the unit Reynolds number $Re_{e,1}$ of the flow at the outer boundary of the boundary layer continuously increase on the active part of the trajectory. On the other hand, this growth is somewhat restrained by the increasing values of the Mach numbers M_e at the outer boundary of the boundary layer. Figure 10(b) illustrates the influence of spherical bluntness on the position of the beginning of the laminar-turbulent transition zone, which shows the calculated dependences for the local friction coefficient C_f along the length of the head part at $M_\infty=1.8$. Curve 1 corresponds to a pointed head part, curve 2 corresponds to a spherical bluntness with radius $R=4$ millimeters. The closeness of curves 1 and 2 indicates a slight influence of this spherical bluntness on the position of the

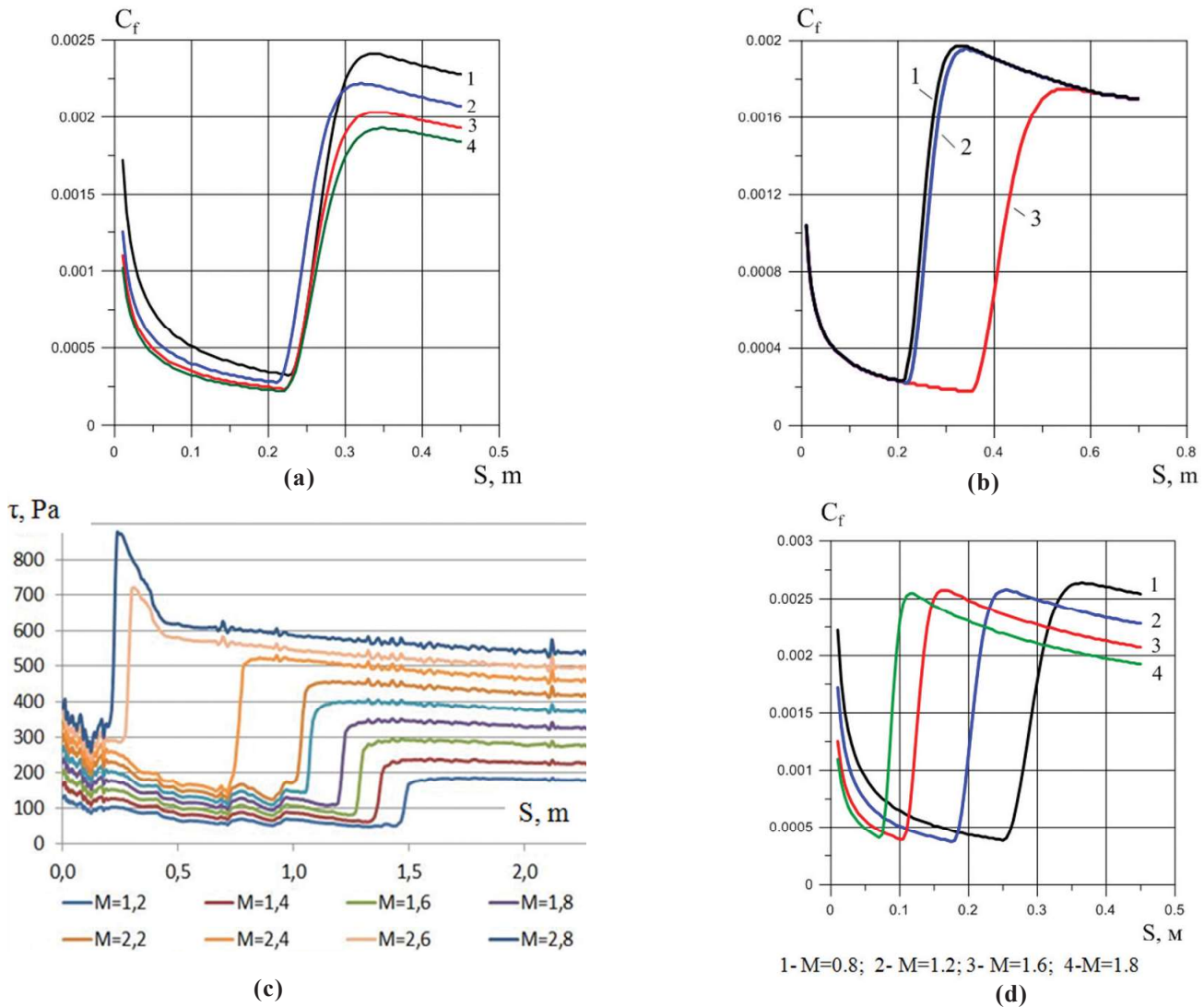


Figure 10. Change in the characteristics of aerodynamic friction and flow regime in the boundary layer along the length of the streamlined surface, a) distribution of the local friction coefficient C_f along the head part (1- $M_\infty=0.8$; 2- $M_\infty=1.2$; 3- $M_\infty=1.6$; 4- $M_\infty=1.8$); (b) shift of the beginning of the transition with an increase in the Mach number from $M_\infty=1.8$ (2) to $M_\infty=6.0$ (3); (c) distribution of shear stress τ along the length of the head part according to the results of numerical calculation; and (d) local friction coefficient C_f without taking into account the change in the unit Reynolds number.

beginning of the transition at $M_\infty=1.8$. At the same time, curve 3 shows the shift of the beginning of the transition on the head part downstream at the Mach number of the of the counterflow $M_\infty=6.0$ and maintaining the value of the bluntness radius $R=4.0$ mm.

When the simulation by the ANSYS CFX software package and γ - $Re_{\theta,t}$ SST turbulence model^{5,30}, recommendations were used for choosing the Reynolds number of the beginning of the transition along the thickness of the momentum loss $Re_{\theta,t}$ during the flight of bodies in the atmosphere⁵ and the characteristics of the atmospheric turbulence intensity along the height³¹. Turbulence intensity at the “Enter” boundary (Fraction Intensity) was 0.1. The calculations were carried out at flow parameters corresponding to standard atmospheric conditions. Mach numbers were modeled by changing the velocity of the oncoming flow within $0.1 < M_\infty < 2.8$. This was accompanied by a proportional change in the values of the unit Reynolds number of the oncoming flow within $2.3 \cdot 10^6 \leq Re_{e,1} \leq 6.5 \cdot 10^7$. In Fig. 10(c) shows the results of numerical calculations of shear

stress along the length of the head part. It can be seen that at the same Mach numbers $M_\infty=1.2$; $M_\infty=1.6$; $M_\infty=1.8$, the zone of the laminar boundary layer has a much larger extent compared to the results of calculations by the integral method using flight data on the transition, Fig. 10(a).

As the Mach numbers of the counterflow increase, the beginning of the laminar-turbulent transition zone noticeably shifts towards the nose of the head part. A similar result was obtained when determining the beginning of a laminar-turbulent transition based on the integral method using a correlation dependence generalizing flight experiments on Mach numbers M_e at a constant value of the unit Reynolds number $Re_{e,1}$ (Fig. 2, Tab. 1, correlation 4). Thus, the influence of a change in the unit Reynolds number $Re_{e,1}$ on the value of the Reynolds number $Re_{e,tr}$ at the beginning of the transition was excluded. In Fig. 10(d) shows the distribution of the local coefficient of friction C_f along the length S of the head part calculated by the integral method in the absence of the influence of the unit Reynolds number $Re_{e,1}$. Two points should

be noted. First, it can be seen that with an increase in the Mach number M_∞ of the counterflow, the beginning of the laminar-turbulent transition zone also shifts quite noticeably towards the nose of the head part. In this case, the absence of growth of unit Reynolds numbers $Re_{e,1}$ is manifested, which results in an accelerated advancement of the beginning of the laminar-turbulent transition zone to the toe of the streamlined body. Secondly, the length of the section of the head part, falling on the transition curves with the same Mach numbers of the counterflow $M_\infty = 1.2; 1.6; 1.8$ in the numerical calculation turned out to be approximately twice as large. This, apparently, is a manifestation of the lack of influence of compressibility on the transition in the indicated range of Mach numbers. The first noted point indicates that the reason for the accelerated reduction in the length of the laminar section in the numerical calculation using the γ - Re_{θ} SST model of the laminar-turbulent transition³⁰ is the absence in its empirical correlations of the mechanism for suppressing the influence of the input small-scale turbulence on the formation of instability waves in the boundary layer with increasing unit number Reynolds number of the oncoming flow. This model has proven itself well in calculating the flow around subsonic and transonic airfoils for various purposes at free flow turbulence levels from 0.1 to 1 % and higher³⁰. The imperfection of this transition model at low levels of free flow turbulence intensity is indicated in studies^{9,10,32}.

4. DISCUSSION

Numerical modeling of the aerophysical characteristics of axisymmetric bodies of rotation based on existing software systems has an undeniable advantage over integral methods for their calculation. In particular, in the presence of such structural elements as blunting of the head part, plumage, bottom part, perforated by nozzles or jets of a running engine. At the same time, the reliability of the obtained simulation results is not guaranteed due to the lack of necessary data on the transient regimes of near-wall flows under conditions of significant changes in velocity and flight altitude. In order to develop reliable transient models within the framework of existing and newly developed CFD codes, the results of full-scale flight tests are needed. In this study, an attempt is made to generalize some known results of flight experiments on laminar-turbulent transition on axisymmetric bodies of rotation in the range of sub-, trans-, and supersonic velocities. These data are presented as a series of correlation dependences that determine the values of the Reynolds numbers of the beginning of the laminar-turbulent transition on sharp cones depending on the Mach number and unit Reynolds number at the outer boundary of the boundary layer. The obtained correlation dependences, taking into account corrections for spherical bluntness, were used in calculating the aerophysical characteristics on the head part of a supersonic axisymmetric body of rotation of the type of an uncontrolled rocket projectile at velocities of $0.1 \leq M_\infty \leq 2.5$ and flight altitudes $H \leq 6300$ meters. As shown by the results of the work, integral methods for calculating the friction and heat transfer of boundary layers^{18,25} using the intermittency function^{19,27-28} and flight data on the laminar-turbulent transition^{6,7,19} make it possible to create effective algorithms

for studying aero physical characteristics on the head parts of supersonic axisymmetric bodies of rotation directly on the calculated trajectories.

Taking into account the mutual advantages and disadvantages of numerical modeling and integral methods, it is proposed to calculate the aero physical characteristics of near-wall high-Reynolds flows on axisymmetric bodies of rotation of the type of an uncontrolled rocket projectile under trajectory flight conditions with significant changes in velocity and altitude in a combined way. The proposed concept is as follows. Using existing software systems, numerically calculate the coefficients of aerodynamic forces and moments for a series of Mach numbers of the oncoming flow M_∞ under standard atmospheric conditions. Perform the calculation of a number of flight trajectories in the first approximation together with the calculation of aerophysical characteristics on the head part of the body of rotation. Calculations of aerophysical characteristics should be carried out by integral methods using correlations of flight data on the beginning of the laminar-turbulent transition and the intermittency function of the boundary layer. At the same time, for the selected series of trajectory points, fix the values of the Mach numbers M_∞ and the unit Reynolds number $Re_{\infty,1}$ of the oncoming flow, as well as the corresponding values of the Reynolds numbers $Re_{e,tr}$ of the beginning and end of the laminar-turbulent transition. For the fixed values of the Mach numbers M_∞ and Reynolds numbers $Re_{\infty,1}$ of the oncoming flow, recalculate the aero physical characteristics using software packages using the obtained values of the Reynolds numbers of the laminar-turbulent transition. Using the obtained values of the coefficients of aerodynamic forces and moments for a series of Mach numbers of the oncoming flow M_∞ on the flight trajectories, perform the final calculation of the trajectories.

5. CONCLUSIONS

A technique has been developed for calculating friction and heating on the surface of supersonic bodies of revolution using a number of well-known integral methods for inviscid flows and viscous near-wall flows that take into account intermittency, compressibility, pressure gradient, and non isothermality of the boundary layer. By means of well-known flight experiments, correlations were obtained for the Reynolds numbers of the beginning of the transition on sharp cones. A method for determining corrections to them by the relative increment of entropy on a shock wave for bodies of revolution with a spherical blunt head part is proposed and implemented. On the example of a supersonic unguided rocket, the possibility of using the developed method for calculating aerodynamic friction and heating of axisymmetric bodies of revolution together with the calculation of the flight trajectory is shown. The flow parameters required for this at the outer boundary of the boundary layer were calculated by solving the equation for the perturbation potential of the velocity of a compressible fluid in a linear approximation using the method of sources and known isentropic relations. The flow regimes in the boundary layer were determined based on the values of the intermittency function of the boundary layer. The values of the intermittency function were calculated from the dependency tested in the course of flight experiments.

The presence of a successive series of flow regimes such as laminar regime, laminar-turbulent transition, turbulent regime, relaminarization (reverse transition), again laminar regime and repeated laminar-turbulent transition has been established. The dependences of the coefficients of friction and heat transfer, heat fluxes and surface temperature along the length of the head part of the projectile during flight along the trajectory under conditions of changing flow regimes, compressibility and non-isothermal boundary layer are determined. Calculations of the projectile surface temperature were carried out by numerically solving the differential equation for heating a “thin wall”. The turbulent viscosity scaling with respect to the intermittency function based on the empirical model of Chen and Tyson²⁷ in the Narasimha concept²⁸ modified in the course of flight experiments¹⁹ can be used for both forward and reverse transitions on the head parts of axisymmetric supersonic bodies of revolution such as uncontrolled rocket projectile. Integral methods, together with flight data on the laminar-turbulent transition, can be used to test existing and newly created turbulence models for CFD codes.

REFERENCES

1. Fedaravicius, A.; Kilikevicius, S.; Survila, A.; Patasiene, L. Analysis of aerodynamic characteristics of the rocket-target for the stinger system. *Problems of Mechatronics Armament Aviation Safety Engineering*, 2016, **7**(1), 7–16. doi: 10.5604/20815891.1195197.
2. Coyle, C.J.; Sifton, S.I. CFD aerodynamic characterisation of a high maneuverability airframe. In 33rd AIAA Applied Aerodynamics Conference, 22-26 June, 2015, Dallas, TX, Paper: AIAA 2015-3015, 2015, 1-15. doi: 10.2514/6.2015-3015.
3. Peng, J.; Zhao, L.; Jiao, L. Numerical simulations on aerodynamic characteristics of a guided rocket projectile. In Proceedings of the 3rd International Conference on Materials Engineering, Manufacturing Technology and Control (ICMEMTC 2016), 27-28 February, 2016, Taiyuan, China, Atlantis Press, 2016, 1004-1007. doi: 10.2991/icmemtc-16.2016.199.
4. Shyiko, O.M.; Pavlyuchenko, A.M.; Skorik, A.V.; Obukhov, O.A. & Kopylyk, I.V. Calculation of the aerodynamic characteristics of supersonic axisymmetric feathered bodies of rotation. *Aerospace Tech. Technol.*, 2019, **2**, 4–17. doi: 10.32620/aktt.2019.2.01.
5. Langtry, R.B. A Correlation-based transition model using local variables for unstructured parallelized CFD code. University of Stuttgart. 2006. PhD. Thesis. 1-101. doi: 10.18419/opus-1705
6. Fisher, D.F. & Dougherty, N.S. In-flight transition measurement on a 10°. Cone at Mach Numbers from 0.5 to 2.0. Paper: *NASA-TP-1971*, 1982, 1-142. <https://ntrs.nasa.gov/api/citations/19820018351/downloads/19820018351.pdf>
7. Beckwith, I.E.; Harvey, W.D.; Harris, J.E. & Holley, B.B. Control of supersonic wind-tunnel noise by laminarization of nozzle-wall boundary layers. Paper: *NASA-TM-X-2879*, 1973, 1-57. <https://ntrs.nasa.gov/api/citations/19740003006/downloads/19740003006.pdf>
8. Potter, J.L. Boundary layer transition supersonic cones in aerobalistic range. *AIAA J.*, 1975, **13**(3), 270-277. doi: 10.2514/3.49692.
9. Boyko, A.V.; Kirilovskiy, S.V.; Maslov, A.A. & Poplavskaya, T.V. Engineering modeling of the laminar-turbulent transition: Achievements and problems (Review). *J. Appl. Mech. Tech. Phys.*, 2015, **56**(5), 761-776. doi:10.1134/S002189441505003X.
10. Risius, S.; Costantini, M.; Koch, S.; Hein, S. & Klein, C. Unit Reynolds number, Match number and pressure gradient effects on laminar-turbulent transition in two-dimensional boundary layers. *Exp Fluids.*, 2018, **59**(5), 1-29. doi: 10.1007/s00348-018-2538-8.
11. Ermolaev, Y.G.; Kosinov, A.D.; Semenov, A.N.; Semionov, N.V. & Yatskikh, A.A. Effect of unit Reynolds number on the laminar-turbulent transition on a swept wing in supersonic flow. *Thermophys. Aeromechanics.*, 2018, **25**(5), 685-691. doi: 10.1134/S0869864318050025.
12. Zhong, X. & Lei, J. Numerical simulation of nose bluntness effects on hypersonic boundary layer receptivity to freestream disturbances. In 41st AIAA Fluid Dynamics Conference and Exhibit, 27-30 June, Honolulu, 2011, 1-29. doi: 10.2514/6.2011-3079.
13. Alexandrova, E.A.; Novikov, A.V.; Utyuzhnikov, S.V. & Fedorov, A.V. Experimental study of laminar-turbulent transition on the blunted cone. *J. Appl. Mech. Tech Phys.*, 2014, **55**(3), 375-385. doi:10.1134/S0021894414030018.
14. Vaganov, A.; Noev, A.; Radchenko, V.; Skuratov, A. & Shustov, A. Laminar-turbulent transition reversal on blunt ogive body of revolution at hypersonic speeds. *Proc. IMechE Part G: J. Aerosp. Eng.*, 2020, **234**(1) 102–108. doi: 10.1177/0954410018788737.
15. Stetson, K. Nosetip bluntness effects on cone frustum boundary layer transition in hypersonic flow. AIAA Paper 83-1763, 1983, 1-18. doi: 10.2514/6.1983-1763.
16. Kara, K.; Balakumar, P. & Kandil, O.A. Effects of nose bluntness on hypersonic boundary-layer receptivity and stability over cones. *AIAA J.*, 2011, **49**(12), 2593-2606. doi:10.2514/1.J050032.
17. Wagner, A.; Laurence, S.; Schramm, J. & Hannemann, K. Experimental investigation of hypersonic boundary-layer transition on a cone model in the High Enthalpy Shock Tunnel (HEG) at Mach 7-5. In 17th AIAA International Space Planes and Hypersonic Systems and Technologies Conference., 11-14 April 2011, San Francisco, California, AIAA Paper 2374, 2012, pp.1-9. doi:10.2514/6.2011-2374.
18. Kutateladze, S.S. & Leontiev, A.I. Heat and mass transfer and friction in a turbulent boundary layer. *Energoatomizdat, Moscow*, 1985, pp. 320.

- <https://archive.org/details/1972-kutateladze-leontyev-nasa-tt-f-805>.
19. Leontiev, A.I. & Pavlyuchenko, A.M. Investigation of laminar-turbulent transition in supersonic boundary layers in an axisymmetric aerophysical flight complex and in a model in a wind tunnel in the presence of heat transfer and suction of air. *J. High Temp.*, 2008, **46**(4), 542–565. doi:10.1134/S0018151X08040159.
 20. Berry, S.; Kimmel, R. & Reshotko, E. Recommendations for hypersonic boundary layer transition flight testing. In 41st AIAA Fluid Dynamics Conference and Exhibit, 27-30 June, Honolulu, Hawaii, Paper: AIAA 2011-3415, 2011, pp. 1-20. doi: 10.2514/6.2011-3415.
 21. Schneider, S.P. Flight data for boundary-layer transition at hypersonic and supersonic speeds. *J. Spacecr. Rockets.*, 1999, **36**(1), 8-20. doi: 10.2514/2.3428.
 22. Malik, M.R. Prediction and control of transition in supersonic and hypersonic boundary layers. *AIAA J.*, 1989, **27**(11), 1487-1493. doi: 10.2514/3.10292.
 23. Gaponov, S.L. & Maslov, A.A. Development of disturbances in compressible flows. Novosibirsk: Nauka, 1980, pp.149.
 24. Krasnov, N.F. Aerodynamics. Textbook for technical colleges. Moscow, 1976, pp. 384.
 25. Kutateladze, S.S. Fundamentals of the theory of heat transfer. Atomizdat, Moscow, 1979, pp. 416.
 26. Emmons, H.W. The laminar-turbulent transition in a boundary layer Part I. *J. Aeronaut. Sci.*, 1951, **18**(7), 490-498. doi: 10.2514/8.2010.
 27. Chen, K.K. & Thyson N.A. Extension of Emmons spot theory to flow on blunt bodies. *AIAA J.*, 1971, **9**(5), 821-825. doi: 10.2514/3.6281.
 28. Narasimha, R. The laminar-turbulent transition zone in the boundary layer. *Prog. Aerosp. Sci.*, 1985, **22**(1), 29-80. doi: 10.1016/0376-0421(85)90004-1.
 29. Dullum, O. The rocket artillery reference book. FFI-rapport 2009/00179. Norwegian Defence Research Establishment (FFI), 2010, pp. 178.
 30. Menter, F.R.; Langtry, R. & Völker, S. Transition modelling for general purpose CFD codes. *Flow Turbul. Combust.*, 2006, **77**, 277-303. doi: 10.1007/s10494-006-9047-1.
 31. Otten, L.J.; Pavel, A.L.; Rose, W.C. & Finley, W.E. Atmospheric turbulence measurements from a subsonic aircraft. *AIAA J.*, 1982, **20**(5), 610-611. doi: 10.2514/3.51118.
 32. Matyushenko, A.A.; Kotov E.V. & Garbaruk A.V. Calculations of the airfoil profile flow using two-dimensional RANS: An analysis of the reasons for the accuracy decrease. *Simul. Physl. Process.*, 2017, **10**(1), 20-30. doi: 10.1016/j.spjpm.2017.03.004.

CONTRIBUTORS

Dr Oleksandr M. Shyiko obtained PhD in Technical Sciences from the National Technical University “Kharkiv Polytechnic Institute”, Kharkiv, Ukraine, specialising in Dynamics and Strength of Machines. He worked as an Associate Professor at the Sumy State University and until recently at the Sumy National Agrarian University. He also worked as a Senior/Leading Researcher at the Research Center of the Missile Forces and Artillery, Sumy, Ukraine, focusing on research in applied aerodynamics and ballistics. His areas of research interest include: Vibrations of machines, aerodynamics, external ballistics.

Contribution in the current study: Development of computational models, algorithm and computational program, calculations, analysis of the obtained data, data visualization, textwriting and editing.

Dr Olexii A. Obukhov obtained PhD from the Odessa National Academy of Food Technologies, Odessa, Ukraine, specialising in refrigeration, vacuum and compressor engineering, and air conditioning systems. Currently, he is an Associate Professor with the Department of Physics at the Sumy National Agrarian University. His areas of research interest include: Aerodynamics, heat transfer, external ballistics. He resides in Sumy, Ukraine.

Contribution in the current study: Computational modeling of the aerophysical characteristics, text editing.

Dr Igor V. Kopylyk obtained PhD in Physical and Mathematical Sciences. Currently, he is working as Head of the Department of Applied Mathematics and Complex Systems Modeling, Sumy State University, Sumy, Ukraine. His areas of research interest include: Solid state physics, aerodynamics and ballistics.

Contribution in the current study: Investigation, software, verification, supervision